Biomaterials 149 (2017) 51–62

Contents lists available at ScienceDirect

Biomaterials

journal homepage: www.elsevier.com/locate/biomaterials

Three-dimensional piezoelectric fibrous scaffolds selectively promote mesenchymal stem cell differentiation

Sita M. Damaraju [a], Yueyang Shen [b], Ezinwa Elele [b], Boris Khusid [b], Ahmad Eshghinejad [c], Jiangyu Li [c, d], Michael Jaffe [a], Treena Livingston Arinzeh [a, *]

[a] Department of Biomedical Engineering, New Jersey Institute of Technology, Newark, NJ 07102-1982, USA
[b] Department of Chemical, Biological and Pharmaceutical Engineering, New Jersey Institute of Technology, Newark, NJ 07102-1982, USA
[c] Department of Mechanical Engineering, University of Washington, Seattle, WA 98195, USA
[d] Shenzhen Key Laboratory of Nanobiomechanics, Shenzhen Institutes of Advanced Technology, Chinese Academy of Sciences, Shenzhen, 518055, Guangdong, China

ARTICLE INFO

Article history:
Received 6 July 2017
Received in revised form
8 September 2017
Accepted 17 September 2017
Available online 19 September 2017

Keywords:
Piezoelectric
Scaffold
Tissue engineering
Mesenchymal stem cell
Smart biomaterial
Electrospinning

ABSTRACT

The discovery of electric fields in biological tissues has led to efforts in developing technologies utilizing electrical stimulation for therapeutic applications. Native tissues, such as cartilage and bone, exhibit piezoelectric behavior, wherein electrical activity can be generated due to mechanical deformation. Yet, the use of piezoelectric materials have largely been unexplored as a potential strategy in tissue engineering, wherein a piezoelectric biomaterial acts as a scaffold to promote cell behavior and the formation of large tissues. Here we show, for the first time, that piezoelectric materials can be fabricated into flexible, three-dimensional fibrous scaffolds and can be used to stimulate human mesenchymal stem cell differentiation and corresponding extracellular matrix/tissue formation in physiological loading conditions. Piezoelectric scaffolds that exhibit low voltage output, or streaming potential, promoted chondrogenic differentiation and piezoelectric scaffolds with a high voltage output promoted osteogenic differentiation. Electromechanical stimulus promoted greater differentiation than mechanical loading alone. Results demonstrate the additive effect of electromechanical stimulus on stem cell differentiation, which is an important design consideration for tissue engineering scaffolds. Piezoelectric, smart materials are attractive as scaffolds for regenerative medicine strategies due to their inherent electrical properties without the need for external power sources for electrical stimulation.

1. Introduction

Tissue engineering or regenerative medicine offers a promising approach to repair damaged tissues by combining cells with biomaterials that act as scaffolds to facilitate tissue growth. The biomaterial can be designed to mimic the native tissue extracellular matrix providing appropriate cues for desired cell function. Endogenous electrical fields have been well established during embryonic development, wound healing and limb regeneration (Reviewed in Ref. [1]). The electrical activity generated can be associated with extracellular matrix materials, such as collagens [2] and glycosaminoglycans (GAGs) [3], which display piezoelectric activity. Specifically, they are capable of converting mechanical strain into electrical output. Tissues, such as bone and cartilage, which contain these materials, have been known to display electrical behavior when subjected to loading or deformation [4–6]. Yet, this phenomena of piezoelectricity has largely been unexplored as a potential scaffold strategy in the tissue engineering field (Reviewed in Refs. [7,8]).

The development of smart materials for biological and biomedical applications is an emerging field. Combining biological entities such as DNA, cells or tissues with soft or flexible piezoelectric materials can yield devices that can dynamically sense and adapt to environmental cues with or without the use of external stimuli. Yet flexible, piezoelectric biomaterials have only been in the form of thin-films, tubes, non-woven or aligned fiber membranes, and isolated fibers (Reviewed in Refs. [7,8]), which limits their use for tissue regeneration applications or as *in vitro* tissue

* Corresponding author. Department of Biomedical Engineering, New Jersey Institute of Technology, University Heights, 614 Fenster Hall, Newark, NJ 07102-1982, USA.
E-mail address: arinzeh@njit.edu (T.L. Arinzeh).

https://doi.org/10.1016/j.biomaterials.2017.09.024
0142-9612/

models. For the growth of three-dimensional (3-D) tissues, we have fabricated 3-D piezoelectric fibrous scaffolds made of poly(-vinylidene fluoride – trifluoroethylene) (PVDF-TrFE), which displays the greatest piezoelectric activity of known polymers [9,10], are biocompatible [11,12] and have been shown to stimulate cell function in a variety of cell types [12–19]. Previous studies have reported the fabrication of electrospun PVDF-TrFE fiber based nanogenerators and characterized their piezoelectric properties under compressive loads or displacements [20,21], making them suitable for self-power generators for energy harvesting applications. This level of output also may induce biological activity. The advantage of using PVDF-TrFE fibrous scaffolds is that externally applied electrodes are not needed wherein electrical stimulation can be generated through physiological movement.

In this study, piezoelectric PVDF-TrFE fibrous scaffolds were evaluated for promoting stem cell differentiation and *in vitro* tissue growth as a first study in demonstrating the potential of 3-D flexible smart materials as tissue engineering scaffolds. PVDF-TrFE scaffolds were either electrospun (as-spun) or electrospun and subsequently heat-treated (annealed) to increase the polar/piezoelectric β-phase crystal content and piezoelectric properties. Mesenchymal stem cell (MSC) differentiation towards chondrogenic and osteogenic lineages on these scaffolds was examined in a dynamic bioreactor where cyclic compression was applied at a physiological frequency, activating the piezoelectric properties of the scaffold. Polycaprolactone (PCL), a non-piezoelectric control, was used since PVDF-TrFE cannot be processed into a non-piezoelectric form due to its piezoelectric β-phase content. Although PCL has a different surface chemistry from PVDF-TrFE, PCL was chosen primarily due to its slow degradation rate and ease in fabricating fibrous scaffolds similar in morphology and size to PVDF-TrFE scaffolds. Additionally, PCL is well known for its biocompatibility with many cell types and is in clinical use [22]. We hypothesized that piezoelectric scaffolds undergoing dynamic compression will enhance chondrogenesis and osteogenesis and *in vitro* tissue formation. Findings demonstrated that MSC differentiation was dependent upon the level of piezoelectric activity of the scaffold, where lower levels promoted chondrogenesis and higher levels promoted osteogenesis. Piezoelectric activity promoted greater differentiation as noted by both matrix synthesis and gene expression than mechanical loading alone, demonstrating the effect of electromechanical stimulation on MSC differentiation.

2. Results

2.1. 3-D piezoelectric scaffold fabrication and characterization

3-D scaffolds were prepared using the electrospinning technique. Electrospinning is a dynamic process where an electric field is applied to an ejecting polymer solution resulting in the formation of fibers that collect on a grounded plate. Conventional electrospinning has the limitation of producing two-dimensional (2-D) sheets or membranes however, we were able to fabricate thick, continuous electrospun scaffolds (Fig. 1A) using a two power supply setup, in contrast to the commonly used one power supply setup, where both the spinneret and grounded plate are charged. Electrospun scaffolds can mimic the fibrous extracellular matrix and provide a large surface area, which has been shown to influence cell attachment and protein adsorption [23] (Fig. 1B–D). Depending on the application, scaffolds properties such as porosity, fiber size and orientation can be customized by modifying the electrospinning process parameters and polymer concentration. Micron sized fibers with large interfiber spacing and porosity for cellular infiltration and tissue growth were achieved for both as-spun and annealed PVDF-TrFE and PCL. No statistical differences were detected between the three scaffold groups for fiber diameters, inter-fiber spacing and porosities (Table 1). In addition, air-water contact angle measurements were performed to assess hydrophobicity and no statistical differences were detected between the three scaffold groups.

Scaffolds were characterized for material properties. No significant differences were detected for the tensile Young's moduli between all three groups, however, the ultimate tensile stress was significantly lower for PCL scaffolds compared to PVDF-TrFE scaffolds (Table 1). The ultimate tensile strain was significantly higher for as-spun PVDF-TrFE (125.17 ± 0.21%) compared to other groups demonstrating its relatively high flexibility. All three groups had compressive Young's moduli on the order of kPa demonstrating their relative softness. As determined by fourier transform infrared (FTIR) spectroscopy, x-ray diffraction (XRD), and differential scanning calorimetry (DSC) (Table 1), the annealed PVDF-TrFE had significantly higher piezeoelctric β-phase fraction and crystallinity than as-spun PVDF-TrFE. Annealing is used with PVDF-TrFE films and recently demonstrated with fibers to enhance degree of crystallinity of the β-phase by choosing annealing temperatures above the Curie temperature (T_c) but below the melting temperature (T_m) [24–26]. In this study, 135 °C was chosen as the annealing temperature, which was between T_c at 113 °C and T_m at 147.4 °C for electrospun as-spun PVDF-TrFE scaffolds as determined by DSC.

2.2. Piezoelectric characterization of scaffolds

Electrical output from the bulk scaffold was determined by applying dynamic compression (Fig. 1E–G). In dry conditions, the voltage output increased linearly with increasing level of deformation and increased with frequency for both PVDF-TrFE scaffolds (Fig. 1H&I). Annealed scaffolds had a higher voltage output than as-spun PVDF-TrFE. The electric fields were approximately 20 mV/mm for as-spun and 1 V/mm for annealed PVDF-TrFE, which corresponds to endogenous electrical fields during early development [27]. PCL did not generate any electrical output. For wet conditions, we immersed the scaffold in saline and measured the streaming potential [28] of the surrounding fluid when the scaffolds were subjected to dynamic sinusoidal compression at 1 Hz and a deformation of 10%, which was the same loading condition as the bioreactor. The streaming potential for the annealed PVDF-TrFE was 61.1 ± 1.5 μV, which was significantly higher than the as-spun PVDF-TrFE scaffolds having a streaming potential of 25.2 ± 2.5 μV. No streaming potential was detected for PCL. To our knowledge, this is the first study characterizing the streaming potential generated by fibrous piezoelectric scaffolds. The streaming potentials were similar to values determined for bone [29].

Piezoresponse force microscopy (PFM) was used to demonstrate piezoelectric behavior in the electrospun fibers. We used PFM switching, with the AC excitation voltage applied on top of a DC bias, to examine the ferroelectric polarization switching at three different locations in as-spun and annealed PVDF-TrFE and PCL fibers. As shown in Fig. 2A–D the displacement amplitude and phase response of the PVDF-TrFE fibers manifest the well-known butterfly loop and hysteresis, which is the signature of ferroelectric materials. The annealed fibers exhibited a higher piezoresponse than that of as-spun ones, as shown by the piezoelectric displacements for the annealed (Fig. 2C) and as-spun samples (Fig. 2A). The control non-piezoelectric PCL fibers do not show the characteristic behaviors as expected (Fig. 2E&F).

2.3. MSC chondrogenic differentiation promoted on piezoelectric scaffolds

The piezoelectric scaffolds, as-spun and annealed PVDF-TrFE,

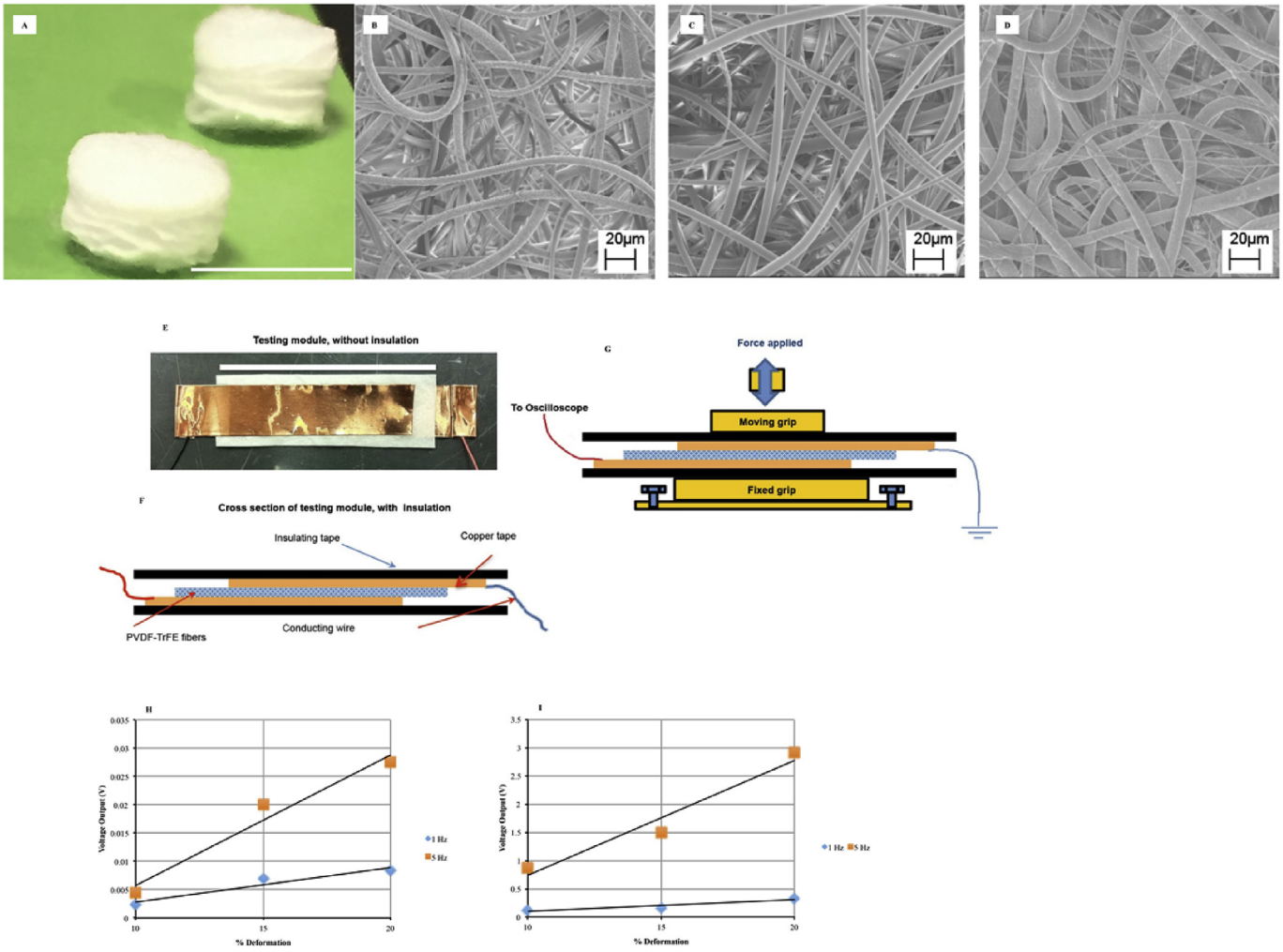

Fig. 1. Picture of piezoelectric scaffolds, approximately 3 mm thick. Scale bar = 6 mm (A). Scanning electron microscope (SEM) images of as-spun PVDF-TrFE (B), annealed PVDF-TrFE (C) and PCL (D) at 2000× magnification. Scale bar = 20 μm. Setup for measuring the electrical output of the piezoelectric scaffolds in dry conditions. (E) Top-down view of the electrical testing setup where the piezoelectric material is sandwiched between copper tape (scale bar = 63.5 mm) (E), side-view (F) and schematic of the testing device where force is applied and recording made by the oscilloscope (G). Corresponding graphs of electric output for as-spun (H) and annealed PVDF-TrFE scaffolds (I) in dry conditions undergoing dynamic compression. Note the difference in the values of the y-axis.

were evaluated for enhancing the chondrogenesis and cartilage matrix formation by human MSCs in comparison to non-piezoelectric PCL as a control. MSCs loaded onto scaffolds in the bioreactor were subjected to dynamic compression at 1 Hz frequency with 10% deformation, which mimics physiological strain and is commonly used for dynamic loading of *in vitro* cartilage [30],

Table 1
Summary of scaffold characterization.

	As-spun PVDF-TrFE	Annealed PVDF-TrFE	PCL
Fiber diameter (μm)	5.9 ± 2.0	6.9 ± 1.7	9.8 ± 3.0
Inter-fiber Space (μm)	81.1 ± 33.8	89.3 ± 28.6	62.2 ± 33.4
Porosity (%)	93 ± 2.7	92 ± 5.5	88 ± 2.0
Water Contact Angle (°)	133.6 ± 2.1	134.3 ± 4.3	135.0 ± 3.5
Tensile Young's Modulus (MPa)	4.0 ± 1.2	5.3 ± 2.3	5.8 ± 1.0
Ultimate Tensile Stress (MPa)	0.68 ± 0.13	0.90 ± 0.28	0.47 ± 0.05*
Ultimate Tensile Strain (%)	125.17 ± 0.21*	17.9 ± 2.6	14.6 ± 1.9
Compressive Young's Modulus (kPa)	5.6 ± 2.3*	10.7 ± 5.7	16.7 ± 4.6
Compressive Stress at 10% strain (kPa)	0.54 ± 0.23	1.25 ± 0.65	1.84 ± 0.53
Melting Temperature (T_m, °C)	147.4 ± 0.4[a]	151.5 ± 0.2[a]	60.3 ± 0.7[a]
Curie Temperature (T_c, °C)	113.1 ± 0.3	125.1 ± 0.5[a]	–
% Crystallinity (X_c)	44.6 ± 4.3[a]	63.8 ± 2.3[a]	36.5 ± 2.0[a]
% Relative β-phase fraction	64 ± 2.8%	75 ± 3.2%[a]	–

Values represent mean ± standard deviation.
*$p < 0.05$ where that particular group is significantly different from other groups.
[a]$p<0.05$ where groups are significantly different.

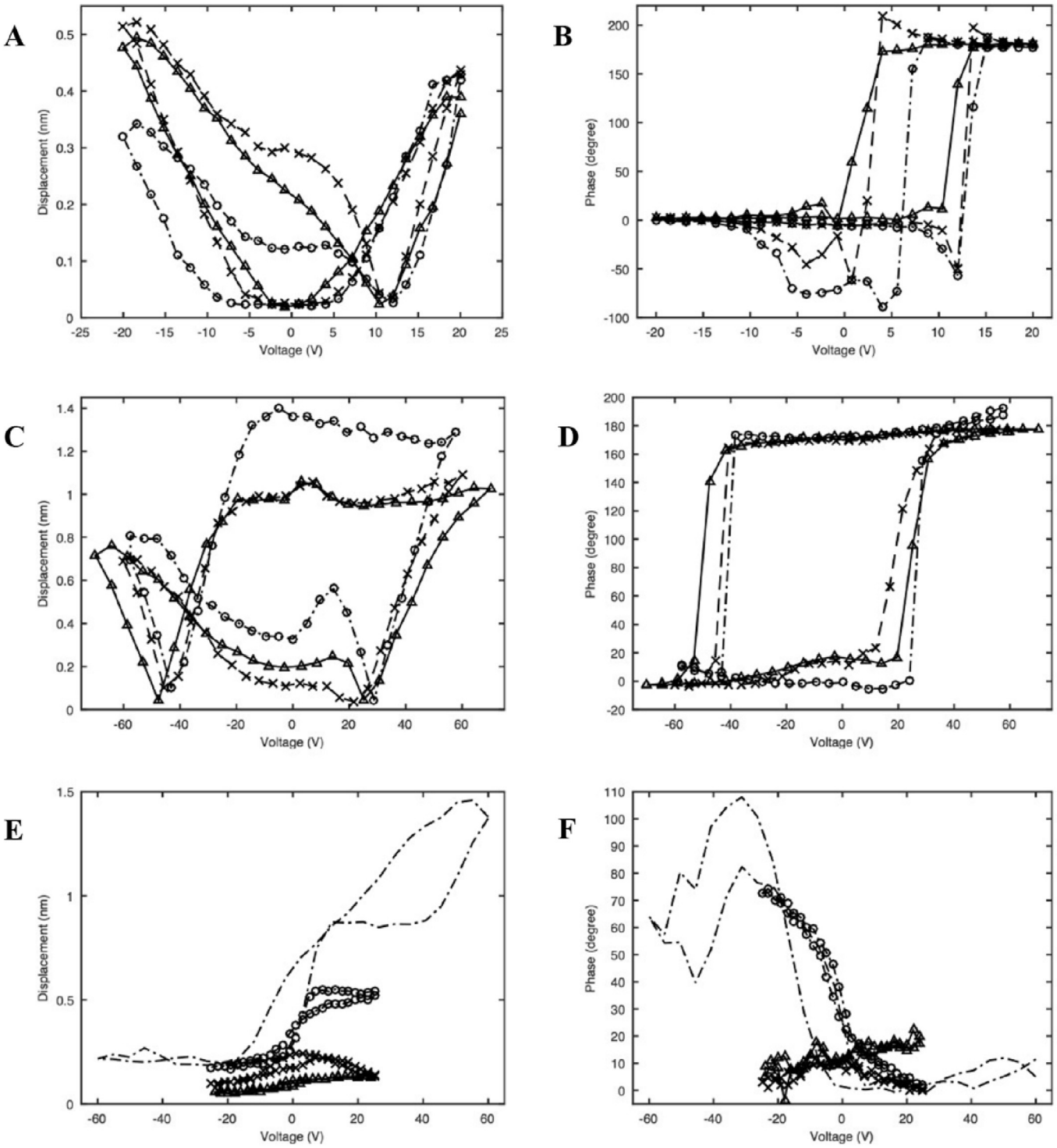

Fig. 2. The displacement amplitude and phase of the PFM switching at different locations on the as-spun PVDF-TrFE (A & B), annealed PVDF-TrFE (C & D) and PCL (E & F) fibers.

with media perfusion and unstimulated controls had media perfusion only for up to 28 days. MSCs were distributed throughout the fibrous constructs, which were cultured in chondrogenic induction medium over a period of 28 days (Fig. S.1). After 28 days in culture, all the constructs had a shiny appearance characteristic of hyaline cartilage as shown in Fig. 3A–C. Histological staining showed a chondrocyte morphology and intense proteoglycan staining as well as collagen type II immunostaining for the as-spun PVDF-TrFE group, which was not readily detected for the other groups in dynamic compression (Fig. 3D–I).

To demonstrate the piezoelectric effects on MSC growth and differentiation, quantitative results are represented as dynamic compression with perfusion (DYN) normalized to perfusion only (PERF) conditions for each scaffold group, unless otherwise noted. Cell number increased at day 14 for the annealed PVDF-TrFE group when undergoing dynamic compression, having the highest fold

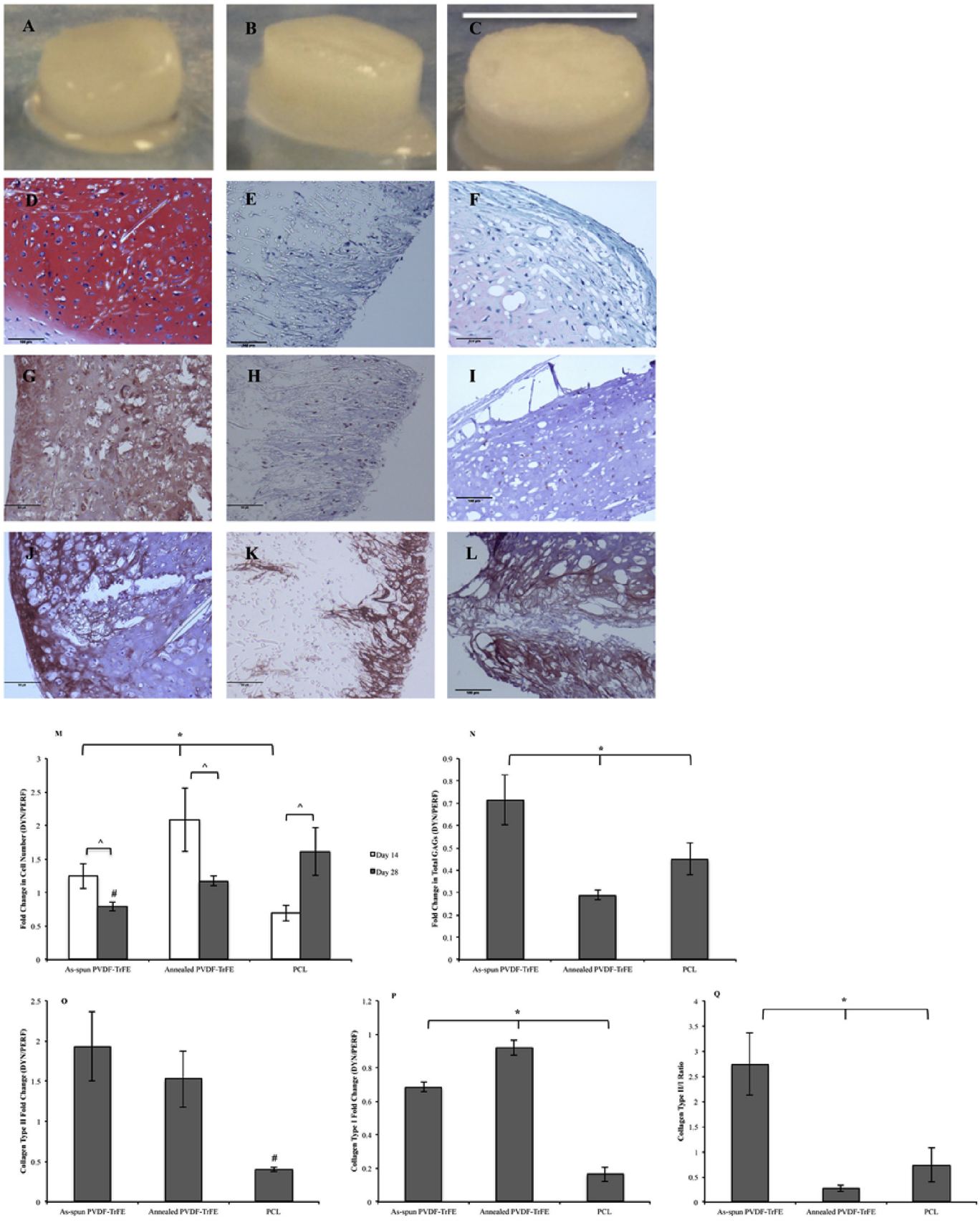

Fig. 3. Representative gross images and histological images of scaffolds after 28 days undergoing chondrogenesis in dynamic conditions. Gross images of as-spun PVDF-TrFE (A), annealed PVDF-TrFE (B) and PCL (C) scaffolds. Histological staining for proteoglycans (safranin-O) (D–F) and immunohistochemical staining for collagen type II (G–I) and collagen type I (J–L) of as-spun PVDF-TrFE (D, G, and J), annealed PVDF-TrFE (E, H, and K) and PCL (F, I and L) scaffolds. (Scale bars: A-C, 6 mm; D-L, 100 mm). Biochemical analysis for MSCs undergoing chondrogenesis on as-spun PVDF-TrFE, annealed PVDF-TrFE and PCL scaffolds. Graphs show cell number (M), total GAG production (N), collagen type II production (O), collagen type I production (P) where dynamic (DYN) is normalized to perfusion only (PERF) groups and collagen types II/I ratio in DYN conditions (Q) at day 28. # $p < 0.05$, significant difference between groups at day 28. ^$p < 0.05$, significant difference between time points. * $p < 0.05$, all three groups are significantly different.

increase over all of the other groups (Fig. 3M). In contrast, for PCL scaffolds, the number of cells decreased by 30% at day 14. By day 28, the fold change in cell number significantly decreased on as-spun and annealed PVDF-TrFE groups by 36% and 44% in comparison to day 14, respectively, with the highest fold increase for the PCL group. Interestingly, the annealed PVDF-TrFE scaffold group had the highest number of cells at days 14 and 28 when compared to as-spun PVDF-TrFE and PCL groups in DYN conditions (Fig. S.2.), indicating the higher piezoelectric activity promotes cell growth. In terms of chondrogenic differentiation, the amount of sulfated GAGs and collagen types II and I were examined at day 28 for each group. The fold change in GAG amount, as an indicator of hyaline cartilage proteoglycan production, was the highest for the as-spun PVDF-TrFE group. Interestingly, for all groups a lower amount was present in DYN conditions as compared to PERF for all groups (<1 fold change). Collagen type II, which is present in hyaline cartilage, and collagen type I, which is indicative of immature fibrocartilage, production was quantified on all three constructs. Both as-spun and annealed PVDF-TrFE scaffold groups promoted greater fold change in collagen type II production as compared to PCL. Fold change in collagen type I synthesis was lower in as-spun PVDF-TrFE and PCL scaffolds (<1 fold change) as compared to the annealed PVDF-TrFE scaffold group, which exhibited no change (~1 fold change) in DYN as compared to PERF conditions. The quality of hyaline cartilage produced is assessed by noting the ratio of collagens types II to I with a higher ratio indicating a more homogenous hyaline cartilage. As-spun PVDF-TrFE group demonstrated a significantly higher collagen types II/I ratio than PCL and annealed PVDF-TrFE groups with the highest ratio in DYN conditions (Fig. 3Q). The ratio of collagens type II/I on the piezoelectric as-spun PVDF-TrFE scaffolds was significantly higher than ratios reported for standard MSC pellet cultures undergoing chondrogenesis [31].

Cartilage tissue specific gene expression was evaluated to assess MSC differentiation on all scaffolds as shown in Table 2 in DYN conditions. Sox9, an early chondrogenic transcription factor, and aggrecan, an early marker for hyaline cartilage proteoglycan, was significantly higher for the PCL group at both days 14 and 28 when compared to as-spun and annealed PVDF-TrFE groups in DYN conditions. However, later stage cartilage markers of collagen types II and IX, which is known to interact with collagen type II [32] and is found in hyaline cartilage, were expressed the highest for the as-spun PVDF-TrFE group as early as day 14 whereas the other groups continued to increase or remain unchanged by day 28, indicating that the as-spun PVDF-TrFE group promoted differentiation earlier than the other groups. Chondroadherin, a mature hyaline cartilage marker, significantly increased for all groups over time. Collagen type I, which is an immature, fibrocartilage marker, and collagen type X, which can be associated with immature as well as hypertrophic chondrocytes, significantly decreased for the as-spun PVDF-TrFE groups by day 28 whereas it increased for the annealed PVDF-TrFE scaffolds and remained unchanged on PCL groups by day 28, further demonstrating a maturation of the cartilage matrix and chondrogenic phenotype for MSCs on as-spun PVDF-TrFE in DYN conditions. Undifferentiated MSCs can express collagen type X mRNA early in cultures that becomes down regulated as MSCs differentiate into chondrocytes [33].

Immunostaining using confocal microscopy (Fig. S.1) confirmed cell attachment as evidenced by actin staining for all of the scaffolds, with more intense actin staining for annealed PVDF-TrFE groups in DYN conditions at day 28. As-spun PVDF-TrFE scaffold group showed intense staining for collagen type II and Sox9. Annealed PVDF-TrFE group had no detectable staining for Sox9 and appeared to have a more punctated collagen type II staining indicating intracellular staining at day 28. Collagen type I staining was intense for annealed PVDF-TrFE. PCL scaffolds had moderate staining for collagen type II and Sox9 and had an intense stain for collagen type I similar to the annealed PVDF-TrFE group at day 28.

2.4. MSC osteogenic differentiation promoted piezoelectric scaffolds

The osteogenic differentiation of MSCs was evaluated on the piezoelectric scaffolds, as-spun and annealed PVDF-TrFE, and compared to non-piezoelectric, PCL, as a control in DYN and PERF conditions. MSCs were cultured in osteogenic induction medium over a period of 28 days. After 28 days in culture, all constructs transitioned to a firm, discrete mass of tissue as shown in Fig. 4A–C. Histological evaluation showed that the annealed PVDF-TrFE group had mineralization staining and intense immunostaining for collagen type I, which appeared to be greater than the other groups (Fig. 4D–F). Fold change in cell number for DYN relative to PERF conditions was high for all three scaffolds as shown in Fig. 4G. Although there were no significant differences noted between all scaffold groups and over time, the as-spun PVDF-TrFE group continued to have a high fold change in cell number. Osteogenic markers of alkaline phosphatase (ALP) activity, mineralization, and osteocalcin were examined. Fold change in ALP activity was

Table 2
Gene expression for chondrogenic samples under dynamic conditions normalized to RPLPO.

		As-spun PVDF-TrFE	Annealed PVDF-TrFE	PCL
SOX9	Day 14	0.15 ± 0.02	0.31 ± 0.04	0.67 ± 0.08$^{\#}$
	Day 28	0.21 ± 0.09	0.27 ± 0.03	0.63 ± 0.19$^{\#}$
Aggrecan	Day 14	1.49 ± 0.06	0.89 ± 0.11	4.68 ± 0.20$^{\#}$
	Day 28	1.13 ± 0.40	1.47 ± 0.43^{a}	3.06 ± 0.53$^{\#,a}$
Collagen type IX	Day 14	2.60 ± 0.22$^{\#}$	0.44 ± 0.04	0.79 ± 0.05
	Day 28	0.54 ± 0.12$^{\#,a}$	1.17 ± 0.43^{a}	0.88 ± 0.17
Collagen type II	Day 14	7.06 ± 0.80$^{\#}$	4.94 ± 0.26	4.06 ± 0.06
	Day 28	5.52 ± 2.16	8.97 ± 2.20^{a}	6.50 ± 1.57^{a}
Chondroadherin	Day 14	0.24 ± 0.04	0.04 ± 0.003$^{\#}$	0.33 ± 0.023
	Day 28	0.36 ± 0.08^{a}	0.40 ± 0.024$^{\wedge,a}$	0.57 ± 0.12$^{\wedge,a}$
Collagen type I	Day 14	31.1 ± 2.68	31.1 ± 5.66	18.1 ± 4.34
	Day 28	11.5 ± 2.83$^{\wedge,a}$	29.7 ± 11.9$^{\wedge}$	23.5 ± 8.50
Collagen type X	Day 14	47.2 ± 2.26$^{\#}$	10.1 ± 3.30	22.3 ± 3.43
	Day 28	20.0 ± 5.06$^{\wedge,a}$	33.3 ± 7.17$^{\wedge,a}$	25.3 ± 4.08

Values represent mean ± standard deviation.
$^{*}p < 0.05$ where all groups are significantly different.
#$p < 0.05$ where that group is significantly different from other groups.
$^{\wedge}p < 0.05$ where those groups are significantly different.
$^{a}p<0.05$ where day 14 is significantly different from day 28 for that particular group.

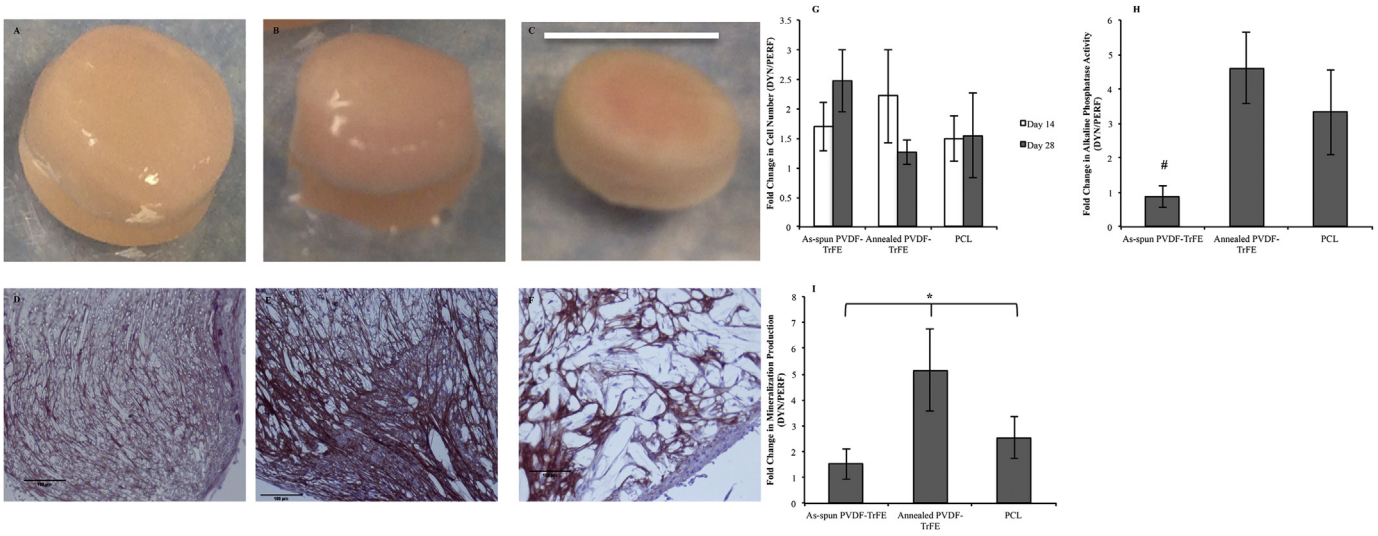

Fig. 4. Representative gross images and histological evaluation of scaffolds after 28 days undergoing osteogenic differentiation in dynamic conditions. Gross images of as-spun PVDF-TrFE (A), annealed PVDF-TrFE (B) and PCL (C) scaffolds. Immunohistochemical staining for collagen type I of as-spun PVDF-TrFE (D), annealed PVDF-TrFE (E) and PCL (F) scaffolds. (Scale bars: A-C, 6 mm; D-F, 100 μm). Biochemical analysis for MSCs undergoing osteogenesis on as-spun PVDF-TrFE, annealed PVDF-TrFE and PCL scaffolds. Graphs show cell number at days 14 and 28 (G), total alkaline phosphatase activity (H), and mineralization (I) where dynamic (DYN) is normalized to perfusion only (PERF) groups. # $p < 0.05$, significant difference between groups at day 28. * $p < 0.05$, all three groups are significantly different.

significantly lower on as-spun PVDF-TrFE scaffolds as compared to annealed PVDF-TrFE and PCL groups at day 28 (Fig. 4H). Fold change and production of matrix mineralization was significantly higher on the annealed PVDF-TrFE group in comparison to PCL and as-spun PVDF-TrFE groups with the least detected for the as-spun group (Fig. 4I). Osteocalcin production and fold change, a protein produced by mature bone cells, was not statistically different amongst all groups (data not shown).

Strikingly, the most pronounced osteogenic markers were expressed at the gene level for the annealed PVDF-TrFE groups in DYN conditions (Table 3). ALP and Runx2, an osteogenic transcription factor, were significantly upregulated for the annealed PVDF-TrFE group compared to as-spun PVDF-TrFE and PCL scaffold groups at day 28. Collagen type I expression decreased by day 28 for all groups, which occurs during the progression of osteogenesis. Osteopontin and osteocalcin, which are both mature bone markers, were expressed the highest on annealed PVDF-TrFE groups and were significantly higher than both groups at day 28, indicating that the annealed PVDF-TrFE scaffolds promoted greater osteogenic differentiation.

Immunostaining using confocal microscopy also supported these findings (Fig. S.2). Cell attachment with intense actin cytoskeleton staining was detected for the annealed PVDF-TrFE scaffolds. Collagen type I and osteocalcin were detected for all three groups however, only annealed PVDF-TrFE scaffolds had intense staining for both proteins throughout the scaffold.

3. Discussion

Piezoelectric, 3-D fibrous PVDF-TrFE scaffolds were evaluated for MSC chondrogenesis and osteogenesis under dynamic loading conditions, where the processing of the scaffolds impacted the level of piezoelectric activity which influenced differentiation. The results demonstrated an increased chondrogenic differentiation of MSCs on as-spun PVDF-TrFE scaffolds, which have lower piezoelectric activity, as determined from GAG, collagen type II to I ratio and gene expression. Additionally, annealed PVDF-TrFE scaffolds, having higher piezoelectric activity, promoted the greatest MSC osteogenic differentiation as noted by increased mineralization and osteogenic gene expression. The preference for a differentiation lineage can be attributed to mechanical loading of the piezoelectric scaffolds, which in turn produces different levels of electrical fields or streaming potentials. The level of piezoelectric activity also can affect cell growth and in turn, alter differentiation. Cells undergoing

Table 3
Gene expression for osteogenic samples under dynamic conditions normalized to RPLPO.

		As-spun PVDF-TrFE	Annealed PVDF-TrFE	PCL
RUNX2	Day 14	0.09 ± 0.01	0.05 ± 0.01	0.10 ± 0.01
	Day 28	0.04 ± 0.01	0.27 ± 0.01$^{\#,a}$	0.09 ± 0.01
Alkaline Phosphatase	Day 14	Not detectable	Not detectable	0.04 ± 0.01$^{\#,a}$
	Day 28	Not detectable	0.05 ± 0.02$^{\#,a}$	0.02 ± 0.002
Collagen type I	Day 14	14.6 ± 3.90	7.77 ± 1.00	9.52 ± 0.92
	Day 28	5.61 ± 1.00^{a}	3.64 ± 1.88	4.99 ± 0.54
Osteocalcin	Day 14	Not detectable	Not detectable	Not detectable
	Day 28	Not detectable	2.07 ± 0.47$^{\#,a}$	0.13 ± 0.04^{a}
Osteopontin	Day 14	0.03 ± 0.01	0.09 ± 0.01$^{\#}$	0.02 ± 0.001
	Day 28	0.04 ± 0.01	0.34 ± 0.08$^{\#,a}$	0.01 ± 0.002

Values represent mean ± standard deviation.
*$p < 0.05$ where all groups are significantly different.
#$p < 0.05$ where that group is significantly different from other groups.
[a]$p<0.05$ where day 14 is significantly different from day 28 for that particular group.

chondrogenic differentiation exposed to higher piezoelectric activity (annealed PVDF-TrFE) and cells undergoing osteogenic differentiation exposed to lower piezoelectric activity (as-spun PVDFT-TrFE) had enhanced growth as early as day 14 and by day 28, respectively, as noted by the increase in fold change in cell numbers where markers for differentiation in these groups were lower. *In vitro* findings suggest the combination of biochemical inductive factors with piezoelectric scaffolds or piezoelectric activity can enhance the proliferation and differentiation of MSCs in a controlled manner, which may be a useful for the development of MSC-based therapies for cartilage and bone applications.

To our knowledge, this is the first study examining MSC chondrogenesis on piezoelectric scaffolds. Protein or actual matrix deposition in these long-term cultures may be a better indicator of chondrogenic differentiation than gene expression since all scaffold groups expressed chondrogenic markers at the gene level. As noted by other studies for MSC chondrogenesis, there is a weak correlation between gene and protein level expression and substantial heterogeneity in the MSC population [34]. For all scaffolds groups, collagen types X and I were detected by gene expression, which suggests the presence of a heterogeneous population of cells within the constructs. Murdoch et al. analyzed cartilage tissue formation from individual clonal populations of MSCs and demonstrated variable differentiation capacity of individual clones [35]. Pelttari et al. compared cartilage formation potential for human MSCs and chondrocytes cultured as pellets and demonstrated that in MSC pellets, premature induction of collagen types I and X genes occurred well before collagen type II was expressed [36]. Following this, a broad range of hyaline cartilage markers together with markers for terminal differentiation were detected. In contrast, hypertrophy related genes were not detectable in chondrocyte pellets when subjected to similar chondrogenic culture conditions as MSCs [36]. In this study, for as-spun PVDF-TrFE group, collagen types I and X gene expression reduced over time as compared to annealed PVDF-TrFE and PCL, suggesting that the as-spun PVDF-TrFE group may be more favorable in reducing this heterogeneity. The protein expression complements this finding by the high collagen type II to I ratio for the as-spun PVDF-TrFE group.

The mechanical stimulus alone, as noted by findings in comparison to the PCL control, did not have a pronounced effect on chondrogenic differentiation as compared to piezoelectric stimulation. In fact, overall matrix synthesis, as measured by GAG content and collagens type I and II production, for MSCs undergoing chondrogenesis due to mechanical stimulation alone decreased, which has been demonstrated by others for MSCs exposed to dynamic compression alone (Reviewed in Ref. [37]). GAG content decreased in dynamic conditions, in terms of fold change when comparing dynamic to perfusion only conditions, for all groups, but to a lesser extent for piezoelectric materials. GAG synthesis was measured on the scaffolds, which may not take into account all GAG synthesis since it has been shown that GAG levels can increase in the media in porous scaffolds and in dynamic loading conditions, failing to attach or accumulate in the extracellular matrix produced by the cells [38]. However, this may be related to the maturation of the cells and/or matrix. Studies have shown that differentiating prior to applying compression reduces heterogeneity in MSC chondrogenic differentiation and thus, improving the expression of chondrogenic markers. It is speculated that by predifferentiating, MSCs differentiate into chondrocyte progenitors, which then respond favorably to dynamic compression by producing a mature cartilage construct [4,39]. Huang et al. have demonstrated that the timing of load initiation does impact biochemical and mechanical properties of the tissue construct [39]. Therefore, delaying dynamic compression after preculture has been shown to promote MSC chondrogenesis by enhancing gene expression, GAG deposition and collagen type II production when compared to dynamic loading initiated soon after scaffold and no dynamic loading groups [37,40].

For osteogenesis, matrix mineralization and alkaline phosphatase activity were at the highest levels for cells on annealed PVDF-TrFE and to a lesser extent due to mechanical stimulus alone, where markers have been shown to be enhanced due to dynamic compression alone for MSC osteogenesis [41]. These findings support that electrical activity had an additive/synergistic effect in promoting differentiation. Previous studies have investigated PVDF, PVDF-TrFE and conducting polymers films for osteogenic differentiation. Dynamically stimulated piezoelectric β-PVDF films demonstrated increased proliferation and differentiation of human adipose stem cells compared to static conditions and non-piezoelectric PVDF films when cultured under similar conditions of piezoelectric β-PVDF, indicating piezoelectric materials can stimulate osteogenesis [42,43]. However, these studies were limited by only examining alkaline phosphatase activity as a marker for differentiation and did not examine changes in the level of piezoelectric activity. An advantage of using PVDF films is having a non-piezoelectric control with the same chemistry as the piezoelectric group. However, films lack the necessary 3-D structure to investigate 3-D organization of cells, tissue or matrix growth or ingrowth and the formation of organized tissue, limiting its potential use for bone tissue engineering or bone repair applications [44–47]. A more recent study has been able to fabricate biocompatible PVDF and PVDF-TrFE membranes with nano pore structures, which were able to support the growth of MC3T3-E1 preosteoblasts and C2C12 myoblast for up to three days in culture [15]. However, nano-size pores limit tissue formation and 3-D growth of cells, which is necessary for chondrogenesis making the 3-D, fibrous PVDF-TrFE scaffold in this study a promising scaffold for investigating MSC differentiation for a variety of tissue engineering applications.

As shown in this study, piezoelectric materials undergoing mechanical loading in ion-containing medium resulted in changes in streaming potential. Streaming potentials or electric potentials were detected in the medium due to fluid flow over the charged piezoelectric surfaces. Electrical or mechanical stimulation, which can be exhibited by changes in streaming potentials, can activate mechanotransduction signaling pathways [48]. Increasing evidence supports that electrical stimulation and piezoelectric materials increase extracellular calcium influx via voltage gated calcium channels present within cell membranes and the release of calcium from intracellular calcium repositories [49–52]. Extensive work by Brighton et al. has shown that electrical fields cause an increase in extracellular calcium influx via voltage gated calcium channels and an increase in intracellular calcium levels in chondrocytes promoting the expression of chondrocyte markers through a calmodulin/calcineurin/NF-AT (nuclear factor of activated T cells) signaling pathway [50,51]. Similarly, electrical stimulation of bone cells promotes osteogenesis through calcium/calmodulin signaling, where they noted both cell proliferation and differentiation. Adipose-derived stem cells (ASCs) exposed to different levels of an electric field had a dose dependent increase in calcium signaling during osteogenic differentiation [53]. MSCs undergoing osteogenesis exposed to an electric field had increased production of ALP and mineralization [54]. A more recent study has demonstrated that electrical stimulation of mouse MSCs significantly enhanced chondrogenic gene expression markers for up to 7 days in culture [55]. Chondrogenesis was driven by intracellular calcium/ATP oscillations and depended on the TGF-β and BMP-2 signaling pathway. Cytoplasmic calcium concentrations have been shown to affect downstream signaling pathways and release of growth factors [56]. Fitzsimmons et al. showed the application of electric field led to an increase in insulin-like growth factor (IGF-II) gene

expression, secretion and receptor expression in osteoblasts. Other signaling molecules/factors, such as cyclic adenosine monophosphate (cAMP) and prostaglandin E_2, were shown to be released following electrical stimulation [51]. Similar phenomena may be occurring with the use of PVDF-TrFE scaffolds. Additional mechanisms such as changes in the amount, conformation and orientation of proteins adsorbed on the charged or piezoelectric surfaces [57] can affect cell behavior.

4. Conclusions

Piezoelectric materials hold promise as a scaffold strategy to enhance tissue formation by providing a smart, electrically active microenvironment without the use of an external power source. Here, we show that piezoelectric materials can be fabricated into flexible, three-dimensional fibrous scaffolds that can be used to stimulate mesenchymal stem cell differentiation and tissue formation when undergoing dynamic loading, which mimics physiological loading conditions found in structural tissues. Findings demonstrate the potential of piezoelectric scaffolds as a viable approach to regenerate tissues using stem cell-based therapies.

5. Materials and methods

Scaffold Fabrication: Fabrication of fibrous scaffolds was accomplished using electrospinning technique. The electrospinning setup consisted of solution of 25 wt/vol% poly (vinylidene difluoride – trifluoroethylene) (65/35, PVDF-TrFE, Solvay Solexis) solution in methyl ethyl ketone (Fisher Scientific). The polymer solution was transferred to a 10 mL syringe fitted with a stainless steel needle. The syringe was placed on a syringe pump (Harvard Apparatus) with a set flow rate of 15 mL/h and a high voltage power supply (Gamma High Voltage Research) was used to apply 25–28 kV to the needle. The electrospun fibers were collected on a charged (2–10 kV) stainless steel plate placed at 35 cm distance away from the tip of the needle. The fibers were spun at room temperature (~20–23 °C) with 15–20% humidity for 15 min for thin scaffolds with ~100–300 μm thickness or 90 min for thicker scaffolds having thicknesses of ~3–4 mm. The scaffolds were placed under vacuum for at least 48 h before further processing. The scaffolds used without further processing were labeled as-spun PVDF-TrFE scaffolds. The annealed PVDF-TrFE scaffolds were achieved by placing the as-spun scaffolds in the oven at 135 °C for 96 h followed by ice water quenching for few seconds. The scaffolds were allowed to dry completely before being used for further tests. As a non-piezoelectric scaffold, polycaprolactone (PCL, MW 80000, Sigma Aldrich) scaffolds were fabricated with 15 wt/wt.% PCL in methylene chloride (Fisher Scientific).

Scaffold Morphology: Fiber morphology, fiber diameter and inter-fiber space were characterized using scanning electron microscopy (SEM, LEO 1530 Gemini). Briefly, samples were sputter coated with gold palladium and viewed using an accelerating voltage of 3–5 kV and a working distance of 4–8 mm. Image J software (National Institutes of Health) was used for all measurements from SEM images using previously reported protocols [58]. Briefly, diameters of at least 80 fibers, 16 each from five samples per group, were measured. Porosity of dry samples was calculated using the following formula [59]:

$$\text{Porosity } (\%) = \left(1 - \frac{\rho_{mat}}{\rho_{raw}}\right) \times 100$$

where ρ_{mat} is the density of the scaffold, which was determined by dividing the mass of the scaffolds by the total volume of scaffold. The raw density, ρ_{raw}, for PVDF-TrFE and PCL is 1.78 and 1.145 gcm^{-3}, respectively.

Water Contact Angle Measurements: Wettability was performed, as previously described [60–62] using a sessile drop water contact measurement using a goniometer built in house. The scaffolds (6 mm diameter) were mounted onto a glass slide using double-sided tape. Water (5 μL) was dropped on the scaffold and the contact angle was recorded (n = 20 per scaffold).

Mechanical Properties: Tensile tests were performed using Instron 3342 single column system (Instron) to determine Young's modulus, ultimate tensile stress and strain for all electrospun scaffold groups. The scaffolds were cut into 70 × 10 mm strips with a testing area of 40 × 10 mm. For each scaffold group, n = 10 samples were tested at a rate of 40 mm/min. Each sample's thickness was measured at three locations along the length of the strip (at the two ends and in the center) and then was averaged to obtain final thickness. All scaffolds were sterilized with 100% ethanol (Fisher Scientific) for 20 min and later rinsed with PBS prior to the mechanical testing. Results are reported as mean ± standard deviation. Unconfined compression tests were performed using dynamic mechanical testing device (DMTA-4, Rheometric Scientific) system to determine compressive Young's modulus. The scaffolds were punched into cylinders with 6 mm in diameter and 3 mm in height. For each scaffold group, n = 10 samples were tested at a strain rate of 0.001% per sec. All the scaffolds were sterilized with 100% ethanol (Fisher Scientific) for 20 min and later rinsed with PBS prior to the mechanical testing.

Fourier Transform Infrared Spectroscopy: Fourier transform infrared spectroscopy (FTIR, Perkin Elmer FTIR-ATR 100 series) was performed for as-spun and annealed PVDF-TrFE scaffolds and the data presented are representative of three independent samples and runs. The samples were scanned from 400 to 1500 cm^{-1} with a resolution of 4 cm^{-1} and total of 40 scans. Previously described procedures were used to determine the relative fraction of β-phase present in each sample [21]. Using characteristic absorption bands of α and β phases at 532 cm^{-1} and 846 cm^{-1}, respectively, and assuming these absorption bands follow Beer-Lambert law with absorption coefficients of $K_\alpha = 6.1 \times 10^4$ and $K_\beta = 7.7 \times 10^4$ cm^2/mol, the fraction of β-phase can be calculated using the following equation:

$$F(\beta) = \frac{X_\beta}{X_\alpha + X_\beta} = \frac{A_\beta}{1.26A_\alpha + A_\beta}$$

where X_α and X_β are the crystalline mass fractions of the α and β phases and A_α and A_β correspond to absorption bands at 532 cm^{-1} and 846 cm^{-1}, respectively.

X-ray Diffraction Analysis: X-ray diffraction (XRD) was performed to confirm the presence of the α and β-phases for as-spun and annealed PVDF-TrFE scaffolds using an X'pert Pro Diffractrometer (Philips PW3050/60). The samples were irradiated with monochromatized Cu Kα (λ = 0.154 nm) X-ray source with a step size (2θ) of 0.02 and scan step time (s) of 1.0. The operating voltage and current used were 45 kV and 40 mA, respectively. The samples were scanned in the 2θ range of 15–45°.

Differential Scanning Calorimetry: Differential scanning calorimetry (DSC; Mettler Toledo Polymer) was used to determine the Curie temperature (T_c), melting temperature (T_m) and Heat of Fusion (ΔH_f) for all samples. The Curie temperature, or Curie transform, is a unique solid–solid phase transition before melting at which the PVDF–TrFE transforms from a ferroelectric (piezoelectric) to a paraelectric (non-piezoelectric) state. The samples underwent a heat-cool-heat temperature cycle program with a heating and cooling rate of 10 °C per minute from −70 °C to +200 °C under nitrogen purge. The DSC data presented were representative of three independent runs. The crystallinity (X_c) of

the samples was calculated using the following equation:

$$X_c(\%) = \frac{H_{fs}}{H_{ft}} \times 100$$

where H_{fs} is the measured heat of fusion for melting of sample, and H_{ft} is the heat of fusion for 100% crystalline PVDF-TrFE, which is 45 Jg^{-1} [13].

Piezoresponse Force Microscope: Piezoresponse force microscope (PFM) was used to evaluate the piezoelectric property of individual fibers for all three groups. Briefly, fibers were electrospun on sputter coated glass slides with gold palladium. The PFM tests were conducted using Asylum Research MFP-3D atomic force microscope. Asylum Research silicon probes with natural frequency of about 70 Hz and stiffness of about 2 N/m were used. The tip radius of the probes was ±10 nm with Ti/lr conductive coating. PFM switching was performed to demonstrate piezoelectric properties by switching the local polarization by applying a triangular sweep of DC bias modulated by square wave signals [63]. On top of the DC bias pulses, small AC probing biases are applied to excite the local piezoelectric response of the samples and measure the induced displacement. Due to the domination of electrostatic effects during the application of DC pulses (ON state), the AC response is measured after each DC pulse (OFF state), in order to characterize the ferroelectricity state in response to the applied DC stimuli.

Measurement of Electrical Output: In dry conditions, scaffolds, approximately 2.5 cm length x 6.4 cm width x ~100–200 μm thickness, were sandwiched between conducting copper tapes (3/4″ width, Mcmaster-Carr, Robbinsville, NJ) which were attached to electrodes. The electrodes were connected to an oscilloscope (Tektronix DPO4000B) for recording the voltage output. Dynamic compression was applied using a Texture Analyzer (TA-XT2, Texture Technologies). Each scaffold was tested at 1 and 5 Hz (sinusoidal waveform) using 10, 15 and 20% deformation.

In wet conditions, each scaffold was cut into 10 mm diameter with 3 mm in thickness disks. The scaffolds were first immersed in 100% ethanol and then rinsed twice and stored in saline until further testing. The disk was placed on a Ag/AgCl electrode (1 mm diameter): one in the center of the sample and the other in the saline bath (reference). The stainless steel platen (connected to the load cell) was used to preload the disk to 5 g force and was defined as the zero strain state. Dynamic sinusoidal tests were performed at 1 Hz and a strain of 10%. The resulting load and streaming potential signals were acquired during the ramp rise and stress relaxation [28].

6. Biological studies

Scaffold Sterilization: All scaffolds were cut into 6 mm diameter disks using a biopsy punch (Miltek, PA, USA). The thickness of scaffold with ~3 mm were chosen for biological studies. The scaffolds were sterilized with 100% ethanol (Fisher Scientific, USA) for 20 min and later air dried in sterile hood overnight prior to cell seeding.

Human Mesenchymal Stem Cells (MSCs) Isolation and Culture: Human MSCs were isolated from whole bone marrow aspirates (Lonza Biosciences, MD), which were collected from the iliac crest of four male and female donors, 18–30 years old. The isolation method has been previously reported [64] The MSCs were cultured on tissue culture polystyrene flasks (Nunc, NY, USA) and maintained at 37 °C and 5% CO_2 in control medium consisting of Dulbecco's Minimum Essential Medium (DMEM; Invitrogen, NY, USA) supplemented with 10% fetal bovine serum (Hyclone, UT, USA), and 1% antibiotic-antimycotic (Invitrogen). MSCs were seeded onto scaffolds at passage three or four.

Bioreactor Overview: Two bioreactors were used in this study. One applied dynamic compression with perfusion (Cartigen 9-X, Instron) through nine wells, which could hold up to nine samples. Cartigen 9-X bioreactor chamber is connected to a load cell (Futek), which is connected to a control box and a laptop computer with software (Instron). The second one, having the same bioreactor design, had perfusion only through nine wells (Cartigen 9-X, Instron), holding up to nine samples. For both bioreactors, perfusion was achieved using Masterflex peristaltic pump systems (Masterflex L/S; Cole Parmer).

Cell Seeding and Bioreactor Conditions: Cells were seeded at 2.0×10^6 cells per mL to each scaffold using a vacuum technique [65]. At 37 °C and 5% CO_2, cells were allowed to attach for 3 h prior to transferring to the bioreactors. The samples (n = 9) were placed in the bioreactor and were subjected to continuous perfusion at a flow rate of 0.5 mL/min for the duration of the experiment of 28 days. Dynamic compression was applied the next day (Day 1) using 10% compressive strain (of scaffolds height) using a sinusoidal waveform at 1 Hz for 3 × (1 h on and 1 h off) per day [30] for up to 28 days. Applied forces and platen displacement were monitored and recorded. Similarly, the samples for perfusion only (n = 9) were loaded in the bioreactor with a continuous perfusion flow rate of 0.5 mL/min and was applied for the duration of the experiment of 28 days. Each scaffold group, as-spun PVDF-TrFE, annealed PVDF-TrFE, and PCL, was investigated at n = 9 per scaffold group per donor. Studies were repeated per donor. The bioreactor conditions were the same for chondrogenic and osteogenic differentiation studies. For chondrogenic differentiation, the chondrogenic medium consisted of high-glucose DMEM (Invitrogen) supplemented with 1 mM sodium pyruvate (Sigma Aldrich), 0.17 mM ascorbic acid-2-phosphate (WAKO Pure Chemicals), 0.1 μM dexamethasone (Sigma Aldrich), 0.35 mM L-proline (Sigma Aldrich), 4 mM L-Glutamine (Invitrogen), 1% antibiotic-antimycotic (Invitrogen), 1% ITS + premix (BD), and 10 ng/mL TGF-β3 (ProSpecbio). For osteogenic differentiation, the osteogenic medium consisted of control medium supplemented with 10 mM beta glycerophosphate (Sigma Aldrich), 50 μM L-ascorbic acid-2-phosphate (WAKO) and 100 nM of dexamethasone (Sigma Aldrich).

Cell Number/Growth: Cell number was determined by DNA quantification using the PicoGreen® ds DNA assay (Invitrogen). Standards were prepared with a known number of MSCs. Standards and samples were lysed in either 3 M guanidine chloride (chondrogenic samples; Sigma Aldrich) or 0.1% triton X-100 (osteogenic samples; Sigma Aldrich). An aliquot of cell lysate was mixed with an equal volume of diluted PicoGreen reagent in 1X TE buffer (1:200, Invitrogen). Fluorescence intensity was measured with a microplate reader (FLX800, Biotek Instruments) at 480 nm excitation and 520 nm emission. A standard curve correlated the fluorescence intensity of standards to known cell number. Based on the standard curve, unknown samples' cell number was determined.

Glycosaminoglycans (GAGs) Production: An aliquot of samples prepared for cell proliferation assay was used to quantify sulfated GAGs using Blyscan Assay kit (Biocolor). An aliquot of the sample was reacted with dye reagent (1,9-dimethylmethyleneblue, DMMB) for 30 min. Bound dye was mixed with dissociation reagent and quantified using spectrophotometer (Emax, Molecular Devices) at 656 nm. The unknown GAGs were determined using a standard curve.

Collagen Types I and II Quantification: Collagen types I and II were quantified using a sandwich enzyme-linked immunosorbent assay (ELISA, Chondrex), according to manufacturer's protocol, which includes guanidine hydrochloride treatment and pepsin digestion. The lysate collected was used for both the collagen type II and type I ELISA using a spectrophotometer (Emax, Molecular Devices) at 490 nm.

Alkaline Phosphatase Activity: Alkaline phosphatase (AP) activity was measured by quantifying the conversion of *para*-nitrophenyl phosphate (Sigma Aldrich) to *para*-nitrophenol (p-NP). Samples were prepared by lysing cells with 0.1% Triton X-100 and incubated at 37 °C for 30 min. The absorbance was read at 405 nm with a microplate spectrophotometer (Emax, Molecular Devices). The AP activity was normalized to cell number determined from the pico green assay and expressed as nmol of p-Np/min/cell.

Osteocalcin: Osteocalcin was measured using an ELISA kit for human osteocalcin (Invitrogen). The assay was performed as per manufacturer's instructions. Absorbance was measured at 405 nm (Emax, Molecular Devices).

Mineralization: Mineralization of the extracellular matrix was measured using a quantichrome calcium detection kit (Bioassay Systems). Briefly, the samples were homogenized and digested in 0.5 N HCL overnight at room temperature. Samples and working solution were mixed and incubated for 3 min. The absorbance was read at 570 nm with a microplate spectrophotometer (Emax, Molecular Devices). Calcium concentrations were determined using a standard curve using known calcium concentrations.

Gene Expression: Samples for gene expression were collected at days 14 and 28. At each time point, gene expression was performed with quantitative reverse transcriptase-polymerase chain reaction (qRT-PCR). RNA was isolated from the samples using RNeasy Micro Kit (Qiagen, Valencia, CA, USA) that includes the homogenization of the sample (QIAshredder, Qiagen, Valencia, CA, USA) and DNA digestion step (RNase Free DNase Set, Qiagen, Valencia, CA, USA). The reverse transcription was performed using previously published protocols [58] using the MX4000 detection system (Stratagene). QuantiTect Assay primers (Qiagen), SOX9, aggrecan, collagen types I, II, IX and X and chondroadherin, were used for analyzing chondrogenic differentiation. For osteogenesis differentiation, collagen type I, RUNX2, alkaline phosphatase, osteocalcin and osteopontin were analyzed. Values were normalized to the housekeeping gene RPLPO (ribosomal protein, large, PO) in the same samples (ΔC_T). Fold change was determined by normalizing dynamic groups to perfusion only groups using $2^{-\Delta\Delta CT}$ [66].

Immunofluorescence Staining for Confocal Imaging: The harvested samples were fixed in 4% paraformaldehyde overnight at 4 °C. The samples were then permeabilized with 0.1% triton-x100 for 15 min at room temperature. As a negative control, scaffolds without cells were immunostained along with harvested samples to ensure lack of non-specific staining. A blocking serum consisting of 5% donkey serum or rabbit serum in 1% bovine serum albumin (BSA) was used to treat samples for 1 h at room temperature to avoid nonspecific antibody binding. For cartilage tissue, the samples were incubated in 1:1000 mouse antihuman collagen type II antibody (Abcam) in 1% BSA overnight at 4 °C For bone tissue, the samples were incubated in 1:1000 rabbit anti-human collagen type I (Abcam) or rabbit antihuman osteocalcin antibody (Abcam) in 1% BSA overnight at 4 °C. After a series of PBS washes, the samples were then incubated in 1:200 secondary antibody (donkey antimouse IgG or rabbit antigoat IgG in1% BSA, Invitrogen) along with 1:100 rhodamine phalloidin (Invitrogen) to view actin for 1 h at room temperature. The nucleus was stained with 4′,6-diamidino-2-phenylindole (DAPI; Invitrogen).

Histology: Harvested samples were fixed in 4% paraformaldehyde overnight at 4 °C and rinsed with PBS. Samples were processed for routine histology, embedded in paraffin, and sectioned. Sections were stained with hematoxylin and eosin (H&E), safranin O for proteoglycans. Paraffin embedded sections were deparaffinized and processed for immunohistochemistry for collagen types I and II (Abcam). Images were taken with an optical microscope (Nikon) at 20× magnification at day 28.

Statistical Analysis: SPSS 20.0 software (SPSS Inc.) was used for statistical analysis of all quantitative data. Results are expressed as mean ± standard deviation. The results were initially tested for normality (Shapiro Wilk test) and Levene's equal variance test. Two-way Analysis of Variance (ANOVA) and the post hoc multiple comparison using Tukey's tests were applied. Probability (p) values < 0.05 were considered statistically significant.

Acknowledgements

The authors would like to thank Martin Garon at Biomomentum, Inc. for the use of their Mach-1 tester to collect streaming potential data of the piezoelectric scaffolds. The authors would like to thank funding support from the National Science Foundation (1006510 and 1610125), National Key Research and Development Program of China (2016YFA0201001) and Science and Technology Plan of Shenzhen City (JCYJ20160331191436180), and the National Science Foundation - Science and Technology Center — Center for Engineering Mechano-Biology (CMMI-15-48571).

Appendix A. Supplementary data

Supplementary data related to this article can be found at https://doi.org/10.1016/j.biomaterials.2017.09.024.

References

[1] M.A. Messerli, D.M. Graham, Extracellular electric fields direct wound healing and regeneration, Biol. Bull. 221 (1) (2011) 79–92.
[2] M. Minary-Jolandan, M.-F. Yu, Nanoscale characterization of isolated individual type I collagen fibrils: polarization and piezoelectricity, Nanotechnology 20 (8) (2009) 1–6.
[3] C.A. Bassett, R.J. Pawluk, Electrical behavior of cartilage during loading, Science 178 (4064) (1972) 982–983.
[4] M.A. Brady, S.D. Waldman, C.R. Ethier, The application of multiple biophysical cues to engineer functional neocartilage for treatment of osteoarthritis (part I: cellular response), Tissue Eng. Part B Rev. 21 (1) (2014) 1–19.
[5] B.M. Isaacson, R.D. Bloebaum, Bone bioelectricity: what have we learned in the past 160 years? J. Biomed. Mater. Res. Part A 95 (4) (2010) 1270–1279.
[6] V.C. Mow, X.E. Guo, Mechano-electrochemical properties of articular cartilage: their inhomogeneities and anisotropies, Annu. Rev. Biomed. Eng. 4 (2002) 175–209.
[7] A.H. Rajabi, M. Jaffe, T.L. Arinzeh, Piezoelectric materials for tissue regeneration: a review, Acta Biomater. 24 (2015) 12–23.
[8] C. Ribeiro, V. Sencadas, D.M. Correia, S. Lanceros-Mendez, Piezoelectric polymers as biomaterials for tissue engineering applications, Colloids Surf. B Biointerfaces 136 (2015) 46–55.
[9] A.J. Lovinger, Ferroelectric polymers, Science 220 (1983) 1115–1121.
[10] H. Ohigashi, M. Koga, M. Suzuki, T. Nakanishi, K. Kimura, N. Hashimoto, Piezoelectric and ferroelectric properties of P (VDF-TrFE) copolymers and their application to ultrasonic transducers, Ferroelectrics 60 (1984) 263–276.
[11] E.G. Fine, R.F. Valentini, R. Bellamkonda, P. Aebischer, Improved nerve regeneration through piezoelectric vinylidenefluoride-trifluoroethylene copolymer guidance channels, Biomaterials 12 (1991) 775–780.
[12] N. Weber, Y.S. Lee, S. Shanmugasundaram, M. Jaffe, T. Livingston Arinzeh, Characterization and in vitro cytocompatibility of piezoelectric electrospun scaffolds, Acta Biomater. 6 (9) (2010) 3550–3556.
[13] Y.-S. Lee, G. Collins, T. Livingston Arinzeh, Neurite extension of primary neurons on electrospun piezoelectric scaffolds, Acta Biomater. 7 (2011) 3877–3886.
[14] Y.S. Lee, T. Livingston Arinzeh, The influence of piezoelectric scaffolds on neural differentiation of human neural stem/progenitors cells, Tissue Eng. Part A 18 (19–20) (2012) 2063–2072.
[15] J. Nunes-Pereira, S. Ribeiro, C. Ribeiro, C.J. Gombek, F. Gama, A. Gomes, D. Patterson, S. Lanceros-Méndez, Poly (vinylidene fluoride) and copolymers as porous membranes for tissue engineering applications, Polym. Test. 44 (2015) 234–241.
[16] G.G. Genchi, L. Ceseracciu, A. Marino, M. Labardi, S. Marras, F. Pignatelli, L. Bruschini, V. Mattoli, G. Ciofani, P (VDF-TrFE)/BaTiO3 nanoparticle composite films mediate piezoelectric stimulation and promote differentiation of SH-SY5Y neuroblastoma cells, Adv. Healthc. Mater. 5 (14) (2016) 1808–1820.
[17] Genchi, Giada Graziana, et al., P (VDF-TrFE)/BaTiO3 Nanoparticle Composite Films Mediate Piezoelectric Stimulation and Promote Differentiation of SH-SY5Y Neuroblastoma Cells, Advanced healthcare materials 5 (14) (2016) 1808–1820.
[18] R. Augustine, P. Dan, A. Sosnik, N. Kalarikkal, N. Tran, B. Vincent, S. Thomas,

P. Menu, D. Rouxel, Electrospun poly (vinylidene fluoride-trifluoroethylene)/zinc oxide nanocomposite tissue engineering scaffolds with enhanced cell adhesion and blood vessel formation, Nano Res. (2017) 1–19.
[19] P. Hitscherich, S. Wu, R. Gordan, L.H. Xie, T. Arinzeh, E.J. Lee, The effect of PVDF-TrFE scaffolds on stem cell derived cardiovascular cells, Biotechnol. Bioeng. 113 (7) (2016) 1577–1585.
[20] J. Chang, M. Dommer, C. Chang, L. Lin, Piezoelectric nanofibers for energy scavenging applications, Nano Energy 1 (3) (2012) 356–371.
[21] L. Persano, C. Dagdeviren, Y. Su, Y. Zhang, S. Girardo, D. Pisignano, Y. Huang, J.A. Rogers, High performance piezoelectric devices based on aligned arrays of nanofibers of poly (vinylidenefluoride-co-trifluoroethylene), Nat. Commun. 4 (2013) 1633.
[22] M.A. Woodruff, D.W. Hutmacher, The return of a forgotten polymer—polycaprolactone in the 21st century, Prog. Polym. Sci. 35 (10) (2010) 1217–1256.
[23] S. Agarwal, J.H. Wendorff, A. Greiner, Use of electrospinning technique for biomedical applications, Polymer 49 (26) (2008) 5603–5621.
[24] K. Lau, Y. Liu, H. Chen, R. Withers, Effect of annealing temperature on the morphology and piezoresponse characterisation of poly (vinylidene fluoride-trifluoroethylene) films via scanning probe microscopy, Adv. Condens. Matter Phys. 2013 (2013).
[25] D. Mao, B.E. Gnade, M.A. Quevedo-Lopez, Ferroelectric properties and polarization switching kinetic of poly (vinylidene fluoride-trifluoroethylene) copolymer, Ferroelectr. - Phys. Eff. (2011) 77–100.
[26] M. Baniasadi, Z. Zu, S. Hong, M. Naraghi, M. Minary-Jolandan, Thermo-electromechanical behavior of piezoelectric nanofibers, ACS Appl. Mater. Interfaces 8 (4) (2016) 2540–3551.
[27] R. Nuccitelli, Endogenous electric fields in embryos during development, regeneration and wound healing, Radiat. Prot. Dosim. 106 (2003) 375–383.
[28] M. Garon, A. Legare, R. Guardo, P. Savard, M.D. Buschmann, Streaming potentials maps are spatially resolved indicators of amplitude, frequency and ionic strength dependant response of articular cartilage to load, J. Biomech. 35 (2002) 207–216.
[29] W. Otter, V.R. Palmieri, D. Wu, K. Seiz, L. McGinitie, G. Cochran, A comparative analysis of streaming potentials in vivo and in vitro, J. Orthop. Res. 10 (1992) 710–719.
[30] R.L. Mauck, M. Soltz, C. Wang, D. Wong, P. Chao, W. Valhmu, C.T. Hung, G.A. Ateshian, Functional tissue engineering of articular cartilage through dynamic loading of chondrocyte-seeded agaros gels, J. Biomech. Eng. 122 (2000) 252–259.
[31] M.B. Mueller, R.S. Tuan, Functional characterization of hypertrophy in chondrogenesis of human mesenchymal stem cells, Arthritis Rheum. 58 (5) (2008) 1377–1388.
[32] D.R. Eyre, T. Pietka, M.A. Weis, J.J. Wu, Covalent cross-linking of the NC1 domain of collagen type IX to collagen type II in cartilage, J. Biol. Chem. 279 (4) (2004) 2568–2574.
[33] F. Barry, R.E. Boynton, B. Liu, J.M. Murphy, Chondrogenic differentiation of mesenchymal stem cells from bone marrow: differentiation-dependent gene expression of matrix components, Exp. Cell Res. 268 (2) (2001) 189–200.
[34] A.J. Cote, C.M. McLeod, M.J. Farrell, P.D. McClanahan, M.C. Dunagin, A. Raj, R.L. Mauck, Single-cell differences in matrix gene expression do not predict matrix deposition, Nat. Commun. 7 (2016).
[35] A.D. Murdoch, T.E. Hardingham, Clonally derived human bone marrow mesenchymal cells show differential collagen II/collagen X expression in chondrogenic culture, Trans. Orthop. Res. 33 (2008) 91.
[36] K. Pelttari, A. Winter, E. Steck, K. Goetzke, T. Hennig, B.G. Ochs, T. Aigner, W. Richter, Premature induction of hypertrophy during in vitro chondrogenesis of human mesenchymal stem cells correlates with calcification and vascular invasion after ectopic transplantation in SCID mice, Arthritis Rheum. 54 (10) (2006) 3254–3266.
[37] C.J. O'Conor, N. Case, F. Guilak, Mechanical regulation of chondrogenesis, Stem Cell Res. Ther. 4 (4) (2013) 61.
[38] A. Cochis, S. Grad, M. Stoddart, S. Farè, L. Altomare, B. Azzimonti, M. Alini, L. Rimondini, Bioreactor mechanically guided 3D mesenchymal stem cell chondrogenesis using a biocompatible novel thermo-reversible methylcellulose-based hydrogel, Sci. Rep. 7 (2017) 45018.
[39] A.H. Huang, M.J. Farrell, M. Kim, R.L. Mauck, Long-term dynamic loading improves the mechanical properties of chondrogenic mesenchymal stem cell-laden hydrogels, Eur. cells Mater. 19 (2010) 72.
[40] A.J. Steward, D.J. Kelly, Mechanical regulation of mesenchymal stem cell differentiation, J. Anat. 227 (6) (2015) 717–731.
[41] R.M. Delaine-Smith, G.C. Reilly, Mesenchymal stem cell responses to mechanical stimuli, Muscles, Ligaments Tendons J. 2 (3) (2012) 169–180.
[42] Ribeiro, Clarisse, et al., Dynamic piezoelectric stimulation enhances osteogenic differentiation of human adipose stem cells, Journal of Biomedical Materials Research Part A 103 (6) (2015) 2172–2175.
[43] J. Pärssinen, H. Hammarén, R. Rahikainen, V. Sencadas, C. Ribeiro, S. Vanhatupa, S. Miettinen, S. Lanceros-Méndez, V.P. Hytönen, Enhancement of adhesion and promotion of osteogenic differentiation of human adipose stem cells by poled electroactive poly (vinylidene fluoride), J. Biomed. Mater. Res. Part A 103 (3) (2015) 919–928.
[44] H.B. Lopes, T. de S Santos, F.S. de Oliveira, G.P. Freitas, A.L. de Almeida, R. Gimenes, A.L. Rosa, M.M. Beloti, Poly (vinylidene-trifluoroethylene)/barium titanate composite for in vivo support of bone formation, J. Biomater. Appl. 29 (1) (2014) 104–112.
[45] P. Martins, S. Ribeiro, C. Ribeiro, V. Sencadas, A. Gomes, F. Gama, S. Lanceros-Méndez, Effect of poling state and morphology of piezoelectric poly (vinylidene fluoride) membranes for skeletal muscle tissue engineering, Rsc Adv. 3 (39) (2013) 17938–17944.
[46] C. Ribeiro, S. Moreira, V. Correia, V. Sencadas, J.G. Rocha, F. Gama, J.G. Ribelles, S. Lanceros-Méndez, Enhanced proliferation of pre-osteoblastic cells by dynamic piezoelectric stimulation, Rsc Adv. 2 (30) (2012) 11504–11509.
[47] J.G. Hardy, R.C. Sukhavasi, D. Aguilar, M.K. Villancio-Wolter, D.J. Mouser, S.A. Geissler, L. Nguy, J.K. Chow, D.L. Kaplan, C.E. Schmidt, Electrical stimulation of human mesenchymal stem cells on biomineralized conducting polymers enhances their differentiation towards osteogenic outcomes, J. Mater. Chem. B 3 (41) (2015) 8059–8064.
[48] R.C. Riddle, H.J. Donahue, From streaming-potentials to shear stress: 25 years of bone cell mechanotransduction, J. Orthop. Res. 27 (2) (2009) 143–149.
[49] I.A. Titushkin, V.S. Rao, M.R. Cho, Mode-and cell-type dependent calcium responses induced by electrical stimulus, Plasma Sci. IEEE Trans. 32 (4) (2004) 1614–1619.
[50] J. Xu, W. Wang, C. Clark, C. Brighton, Signal transduction in electrically stimulated articular chondrocytes involves translocation of extracellular calcium through voltage-gated channels, Osteoarthr. Cartil. 17 (3) (2009) 397–405.
[51] C.T. Brighton, W. Wang, R. Seldes, G. Zhang, S.R. Pollack, Signal transduction in electrically stimulated bone cells, J. Bone & Jt. Surg. 83 (10) (2001) 1514–1523.
[52] G. Ciofani, D. Danti, D. D'Alessandro, S. Ricotti, S. Moscato, G. Bertoni, A. Falqui, S. Berrettini, M. Petrini, V. Mattoli, A. Menciassi, Enhancement of neurite outgrowth in neuronal-like cells following boron nitride nanotube-mediated stimulation, ACS Nano 4 (10) (2010) 6267–6277.
[53] S.D. McCullen, J.P. McQuilling, R.M. Grossfeld, J.L. Lubischer, L.I. Clarke, E.G. Loboa, Application of low-frequency alternating current electric fields via interdigitated electrodes: effects on cellular viability, cytoplasmic calcium, and osteogenic differentiation of human adipose-derived stem cells, Tissue Eng. Part C. Methods 16 (6) (2010) 1377–1386.
[54] S. Sun, Y. Liu, S. Lipsky, M. Cho, Physical manipulation of calcium oscillations facilitates osteodifferentiation of human mesenchymal stem cells, FASEB J. 21 (7) (2007) 1472–1480.
[55] H.J. Kwon, G.S. Lee, H. Chun, Electrical stimulation drives chondrogenesis of mesenchymal stem cells in the absence of exogenous growth factors, Sci. Rep. 6 (2016).
[56] R.J. Fitzsimmons, D.D. Strong, S. Mohan, D.J. Baylink, Low-amplitude, low-frequency electric field-stimulated bone cell proliferation may in part be mediated by increased IGF-II release, J. Cell. Physiol. 150 (1) (1992) 84–89.
[57] N. Barroca, P.M. Vilarinho, A.L. Daniel-da-Silva, A. Wu, M.H. Fernandes, A. Gruverman, Protein adsorption on piezoelectric poly(l-lactic) acid thin films scanning probe microscopy, Appl. Phys. Lett. 98 (13) (2011), 133705.
[58] S. Shanmugasundaram, H. Chaudhry, T.L. Arinzeh, Microscale versus nanoscale scaffold architecture for mesenchymal stem cell chondrogenesis, Tissue Eng. Part A 17 (5–6) (2010) 831–840.
[59] S. Sell, C. Barnes, D. Simpson, G. Bowlin, Scaffold permeability as a means to determine fiber diameter and pore size of electrospun fibrinogen, J. Biomed. Mater. Res. Part A 85A (1) (2008) 115–126.
[60] H. Lee, C.H. Jang, G.H. Kim, A polycaprolactone/silk-fibroin nanofibrous composite combined with human umbilical cord serum for subacute tympanic membrane perforation; an in vitro and in vivo study, J. Mater. Chem. B 2 (18) (2014) 2703–2713.
[61] H.R. Pant, M.P. Neupane, B. Pant, G. Panthi, H.-J. Oh, M.H. Lee, H.Y. Kim, Fabrication of highly porous poly (ε-caprolactone) fibers for novel tissue scaffold via water-bath electrospinning, Colloids Surf. B Biointerfaces 88 (2) (2011) 587–592.
[62] Y. Zhang, H. Ouyang, C.T. Lim, S. Ramakrishna, Z.M. Huang, Electrospinning of gelatin fibers and gelatin/PCL composite fibrous scaffolds, J. Biomed. Mater. Res. Part B Appl. Biomater. 72 (1) (2005) 156–165.
[63] Y. Liu, D.N. Weiss, J. Li, Rapid nanoimprinting and excellent piezoresponse of polymeric ferroelectric nanostructures, ACS nano 4 (1) (2009) 83–90.
[64] S. Haynesworth, J. Goshima, V. Goldberg, A. Caplan, Characterization of cells with osteogenic potential from human marrow, Bone 13 (1) (1992) 81–88.
[65] T.L. Arinzeh, S.J. Peter, M.P. Archambault, C. Van Den Bos, S. Gordon, K. Kraus, A. Smith, S. Kadiyala, Allogeneic mesenchymal stem cells regenerate bone in a critical-sized canine segmental defect, J. Bone & Jt. Surg. 85 (10) (2003) 1927–1935.
[66] K.J. Livak, T.D. Schmittgen, Analysis of relative gene expression data using real-time quantitative PCR and the $2^{-\Delta\Delta C}$T method, Methods 25 (4) (2001) 402–408.